Article

pubs.acs.org/Biomac

pH-Triggered Charge-Reversal Polypeptide Nanoparticles for Cisplatin Delivery: Preparation and In Vitro Evaluation

Yue Huang,[†,‡] Zhaohui Tang,*[,†] Xuefei Zhang,*[,‡] Haiyang Yu,[†] Hai Sun,[†] Xuan Pang,[†] and Xuesi Chen[†]

[†]Key Laboratory of Polymer Ecomaterials, Changchun Institute of Applied Chemistry, Chinese Academy of Sciences, Changchun, 130022, People's Republic of China

[‡]Key Laboratory of Environmentally Friendly Chemistry and Applications of Ministry of Education and Key Laboratory of Polymeric Materials and Application Technology of Hunan Province, Xiangtan University, Xiangtan 411105, People's Republic of China

Supporting Information

ABSTRACT: A series of pH-responsive random copolymer poly(L-glutamic acid-*co*-L-lysine) [P(Glu-*co*-Lys)] were synthesized through the ring-opening polymerization (ROP) of γ-benzyl-L-glutamate *N*-carboxyanhydride (BLG-NCA) and 3-benzyloxycarbonyl-L-lysine *N*-carboxyanhydride (ZLys-NCA) and the subsequent deprotection. The chemical structure of the P(Glu-*co*-Lys)s was confirmed by NMR. Critical aggregation concentration and transmission electron microscopy measurements indicated that the P(Glu-*co*-Lys)s could self-assemble into aggregates in phosphate buffer. The surface charge of P(Glu-*co*-Lys) aggregates was greatly affected by the solution's pH and L-glutamic acid/L-lysine ratio because the carboxyl and amino groups present on the P(Glu-*co*-Lys) aggregates could be protonated or deprotonated to become charged. The pH value of the solution at which the surface charge of the P(Glu-*co*-Lys) aggregates reversed could be manipulated by the feed ratio of BLG-NCA and ZLys-NCA. In vitro methyl thiazolyl tetrazolium assays demonstrated that negatively charged P(Glu-*co*-Lys)s were nontoxic and biocompatible. Positive charged P(Glu-*co*-Lys)s showed some cytotoxicity to Hela cells. Cisplatin (CDDP) was used as a model anticancer drug to evaluate the charge-reversal drug delivery system. By the manipulation of CDDP loading content, the surface charge of the CDDP/P(Glu-*co*-Lys) nanoparticles could be reversed to positive from negative at tumor extracellular pH (pH_e 6.5−7.2). An enhanced drug uptake and inhibition of cancer cell proliferation were observed for the tumoral pH_e triggered charge-reversal CDDP/P(Glu-*co*-Lys) drug delivery system. These indicated that the CDDP/P(Glu-*co*-Lys) nanoparticles could be used as intelligent drug delivery systems for cancer therapy.

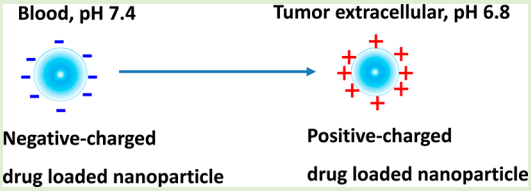

INTRODUCTION

In the past few decades, many delivery systems, such as polymeric micelles, vesicles, liposomes, and nanogels have been exploited for the controlled release of anticancer drugs.[1−4] Stimuli-responsive drug delivery systems have gotten increasing attention for anticancer drugs because they offer a convincing approach to understand the basic principles of drug delivery and to maximize therapeutic activity while minimizing negative side effects.[5] Typical stimuli explored for responsive drug delivery systems can be broadly classified with respect to the biological systems as either internal or external.[6] Representative internal stimuli include pH-shift,[7,8] redox reaction,[9,10] ionic strength,[11−13] enzyme.[14,15] Of these stimuli, pH-responsiveness is one of the most frequently used because obvious pH changes occur within the various tissues and cellular compartments along the endocytic pathway (Table 1).[16] The extracellular pH (pH_e) of normal tissues and blood pH are kept constant at pH 7.4 and their intracellular pH (pH_i) at 7.2.[7] The tumor extracellular environment has a pH of 6.5−7.2. Once being endocytosized, the drug carriers will experience a pH drop from 7.4 to around 6.0 in the early endosomes, with further reduction to pH 5.0 or even lower to 4.5 during progression from late endosomes to lysosomes.[8,17,18] By utilizing the variations in pH values, drug delivery systems have the potential to trigger drug release according to the pH difference.[19−23]

Table 1. pH in Various Tissues and Cellular Compartments in Endocytic Pathway (Adapted from Bae[7] and Pillay et al.[16])

tissue/cellular compartment	pH
extracellular pH of normal tissues	7.4
intracellular pH of normal tissues	7.2
extracellular pH of tumor	6.5−7.2
blood	7.35−7.45
early endosome	6.0−6.5
late endosome	5.0−6.0
lysosome	4.5−5.0

Surface charge has great influence on the uptake of nanocarriers by cells.[24,25] Because cell membranes are negatively charged, positively charged nanocarriers show higher affinity for cell membrane and are expected to be internalized more efficiently than those negatively charged.[26] However,

Received: March 9, 2013
Revised: May 10, 2013
Published: May 11, 2013

positive-charged nanocarriers in the bloodstream have strong nonspecific cellular uptake and interact strongly with serum components, which causes severe aggregation and rapid clearance from circulation and therefore are not suitable for in vivo application.[27,28] In contrast, negative-charged nanocarries have shown potential protein resistance and long circulation for in vivo experiments.[20,29] Therefore, it will make sense to create nanocarriers that are negative-charged during blood circulation, and then transform into a positive-charged form in a tumor.

Considering that the tumoral extracellular environment (pH 6.5−7.2) is more acidic than that of blood (pH 7.4), that positively charged nanocarriers have higher affinity for cell membrane and that negative-charged nanocarries have long circulation in the bloodstream, the strategy, utilizing the unique tumoral extracellular pH as a trigger to reverse the negative-charged nanocarrier to a positive-charged one upon arrival at the acidic tumor sites, have the potential to combine the advantage of positive and negative-charged nanocarriers and improve the targeting efficiency. Bae and co-workers reported an anionic poly(methacryloyl sulfadimethoxine) shielded TAT peptide-based micelle system that could expose TAT at slightly acidic tumor pH.[30] Wang et al. reported a tumor-acidity-activated charge-conversional nanogel that could be transformed from a negatively charged form into a positively charged form in the slightly acidic tumor extracellular environment. The charge conversion enhanced the cellular uptake of the nanogel and promoted cargo release, which led to remarkably enhanced efficiency in killing cancer cells.[27] These studies have demonstrated the feasibility of the tumoral extracellular acidity activated charge-reversal strategy. However, nonbiodegradable polymers such as poly(methacyloyl sulfadimethoxine) and poly(2-aminoethyl methacrylate hydrochloride) were used as pH-responsive materials in these anticancer drug delivery systems.[27,30] These nonbiodegradable polymers may remain in the body and be dealt with as a foreign body, which may result in the formation of pathological tissue and the induction of malignancy.[31] Full biodegradable nanocarriers with tumor-pH_e-activated charge-reversal features for enhanced cellular uptake are highly desired but remain scarcely investigated.

Synthetic polypeptide, one of the most important biodegradable polymers, has found wide uses in biomedical application such as drug delivery, tissue engineering, diagnostics, and biosensors.[32,33] Poly(L-glutamic acid) and poly(L-lysine), as typical polypeptides, have many side pH-responsive groups. Zhang et al. reported the poly(*N*-isopropylacrylamide)-*block*-poly(L-glutamic acid-*co*-L-lysine) PNiPAM(PLG-*co*-PLLys) copolymer was stimuli-responsive to pH variation in aqueous solutions. The unique responsive behaviors of the PNiPAM(PLG-*co*-PLLys) to pH were controlled by the protonation and deprotonation competition between lysine and glutamic acid residues.[34] Lecommandoux and co-workers reported diblock copolymer poly(L-glutamic acid)-*b*-poly(L-lysine) formed pH-sensitive nanoparticles. Schizophrenic vesicles could be reversibly produced as a function of pH in pure water.[35] These inspired us to develop a tumor extracellular acidity activated charge-reversal drug delivery system using pH-responsive polypeptide of L-glutamic acid and L-lysine as a carrier.

Herein, we report on a charge-reversal poly(L-glutamic acid-*co*-L-lysine) [P(Glu-*co*-Lys)] nanocarrier triggered by tumor extracellular acidity for enhanced cellular uptake and anticancer efficiency of anticancer drug. The P(Glu-*co*-Lys) have pH-sensitive side groups of carboxyl and amino. By changing the L-glutamic acid/L-lysine ratio (Glu/Lys) and the *cis*-diaminodichloroplatinum(II) (CDDP) loading content, the surface charge of the CDDP/P(Glu-*co*-Lys) nanoparticles was expected to be reversed to positive from negative when the pH decrease to 6.8 (Tumor extracellular pH) from 7.4 (Blood pH), so that the CDDP/P(Glu-*co*-Lys) nanoparticles have enhanced uptake efficiency and anticancer effect once they arrived at the cancer tissue (Figure 1).

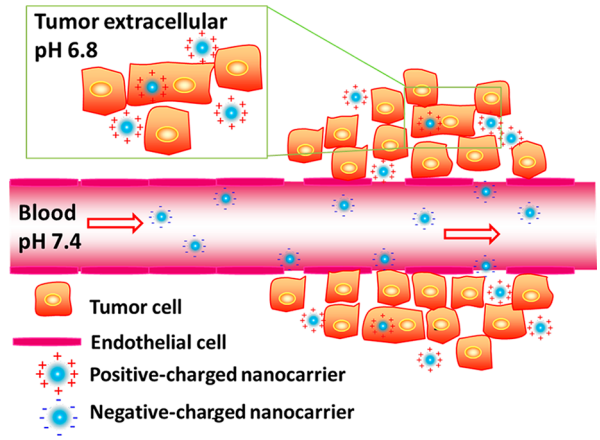

Figure 1. Schematic representation of tumor-pH_e-triggered charge-reversal CDDP/P(Glu-*co*-Lys) nanocarriers that are negative-charged in blood circulation and reach tumors through the leaky vasculature surrounding the tumors where the surface-charge of the nanocarriers were reversed to positive. This enhanced the internalization and anticancer effect of drug-loaded nanocarriers.

EXPERIMENTAL SECTION

Materials. The γ-benzyl-L-glutamate *N*-carboxyanhydride (BLG-NCA) and 3-benzyloxycarbonyl-L-lysine *N*-carboxyanhydride (ZLys-NCA) were synthesized, as described in our previous works.[36] BLG-NCA and ZLys-NCA were recrystallized twice from ethyl acetate before use. Nile red and 3-(4,5-dimethylthiazol-2-yl)-2,5-diphenyl tetrazolium bromide (MTT) were purchased from Sigma-Aldrich. *n*-Hexylamine, anhydrous ether, 33 wt % solution of HBr in acetic acid, and trifluoroacetic acid (TFA) were from Aladdin Industrial Corporation. Dimethyl sulfoxide (DMSO) and dimethyl formamide (DMF) were dried over CaH_2 and distilled before use. *cis*-Diaminodichloroplatinum(II) (Cisplatin, CDDP) was purchased from Shandong Boyuan Chemical Company, China. All the other reagents and solvents were purchased from Sinopharm Chemical Reagent Co. Ltd., China, and used as received.

Synthesis of Poly(L-glutamic acid-*co*-L-lysine) [P(Glu-*co*-Lys)]. P(Glu-*co*-Lys) was prepared through the random copolymerization of BLG-NCA and ZLys-NCA in DMF using *n*-hexylamine as initiator with an 100/1 molar ratio of the total NCA to initiator. Typically, P(Glu-*co*-Lys) copolymer **1** was prepared in the following manner. BLG-NCA (1.56 g, 6.0 mmol), ZLys-NCA (0.45 g, 1.5 mmol) were dissolved in 12 mL of anhydrous DMF under a nitrogen atmosphere. Then *n*-hexylamine (7.65 mg, 0.075 mmol) in anhydrous DMF solution (1.0 mL) was added. The polymerization was performed at 25 °C for 3 days before precipitated into excessive ether. A white solid [poly(BLG-*co*-ZLys)] was obtained after drying under vacuum at room temperature for 24 h. The white solid was dissolved in 10 mL of trifluoroacetic acid and then 3 mL of HBr/acetic acid (33 wt %) was added. The solution was stirred at 30 °C for 1 h before precipitated into excess ether and washed twice with ether. After drying under vacuum, the precipitate was dialyzed with distilled water and freeze-dried to give the P(Glu-*co*-Lys) copolymer **1** in white powders. P(Glu-*co*-Lys) copolymers **2**−**4** were prepared in a similar

dx.doi.org/10.1021/bm400358z | *Biomacromolecules* 2013, 14, 2023−2032

Table 2. Characterization of P(Glu-*co*-Lys) Copolymers[a]

copolymer	feed molar ratio[b]	resultant molar ratio[c]	$M_n \times 10^{-3}$ (g mol^{-1})[d]	PDI[d]	CAC (10^{-3} g L^{-1})	R_h[e] (nm)	R_{TEM}[f] (nm)	zeta potential at pH 6.8 (mV)	zeta potential at pH 7.4 (mV)
1	4:1	4.1:1	17.7	1.22	6.3	96 ± 30	54 ± 13	−26.8 ± 3.6	−30.3 ± 5.3
2	1.5:1	1.5:1	20.2	1.16	11.1	113 ± 20	40 ± 12	−20.9 ± 5.0	−21.8 ± 2.8
3	1:1	0.97:1	18. 5	1.19	40.4	132 ± 33	36 ± 5	−13.4 ± 4.2	−15.5 ± 6.7
4	1:1.5	1:1.4	17.1	1.20	5.4	88 ± 9	41 ± 9	7.1 ± 4.4	4.9 ± 4.0

[a][BLG-NCA + ZLys-NCA]/[*n*-hexylamine] = 100/1. [b]Feed molar ratio of BLG-NCA/ZLys-NCA. [c]Resultant molar ratio of Glu/Lys, determined by ^{1}H NMR based on the intensities ratio of signals at 3.00 ppm (-C$\boldsymbol{H}_2$NH$_2$, k) and 2.40 ppm (HOOCC$\boldsymbol{H}_2$-, f). [d]Determined by GPC. [e]Mean ± standard deviation, determined by DLS. [f]Determined by TEM.

manner except that the amounts of BLG-NCA and BLLys-NCA were changed according to the targeted molar ratio. The results were shown in Table 2. Yield of P(Glu-*co*-Lys) copolymers **1**−**4** was 56.6, 62.5, 64.8, and 58.0%, respectively. ^{1}H NMR (400 MHz, trifluoroacetic acid-*d*, 298 K) of P(Glu-*co*-Lys): δ (ppm) 6.59 (br, -(C═O)N$\boldsymbol{H}$- of Lys unit), 4.59 (br, -C$\boldsymbol{H}$< of Gly unit), 4.38 (br, -C$\boldsymbol{H}$< of Lys unit), 3.00 (br, -C$\boldsymbol{H}_2$NH$_2$ of Lys unit), 2.40 (br, -C$\boldsymbol{H}_2$COOH of Glu unit), 2.07 and 1.92 (br, -C$\boldsymbol{H}_2$CH$_2$COOH of Glu unit), 1.70−1.61 (br, >CHC$\boldsymbol{H}_2$- and >CHCH$_2$CH$_2$C$\boldsymbol{H}_2$- of Lys unit), 1.41−1.32 (br, -C$\boldsymbol{H}_2$CH$_2$CH$_2$NH$_2$ of Lys unit), 1.10−0.95 (br, -C$\boldsymbol{H}_2$- of hexyl group), 0.65−0.55 (br, -C$\boldsymbol{H}_3$ of hexyl group). ^{13}C NMR (75 MHz, trifluoroacetic acid-*d*, 298 K) of P(Glu-*co*-Lys): δ (ppm) 174.8, 169.7, 169.1, 50.3, 49.2, 36.5, 26.9, 26.6, 25.1, 22.1, 18.1.

Characterizations. ^{1}H and ^{13}C NMR spectra were recorded on AV-300 or AV-400 NMR spectrometer (Bruker) at room temperature in trifluoroacetic acid-*d* (TFA-*d*) or deuterated water (D_2O). Gel permeation chromatography (GPC) measurements were conducted on a waters GPC system (Waters Ultrahydrogel Linear column, 1515 HPLC pump with 2414 Refractive Index detector) using NaAc/HAc water solution (pH 7.4) as eluent (flow rate: 1 mL/min, 25 °C, and polyethylene glycol as standards). The zeta potential was measured by Brookhaven instrument (25 °C, concentration: 0.2−0.4 mg/mL, and run 10 times). Dynamic laser scattering (DLS) measurements were performed on a WyattQELS instrument with a vertically polarized He−Ne laser (DAWN EOS, Wyatt Technology). Transmission electron microscopy (TEM) measurements were performed on a JEOL JEM-1011 transmission electron microscope with an accelerating voltage of 100 kV. A drop of solution (0.5 g L^{-1}) was deposited onto a 230 mesh copper grid coated with carbon and allowed to dry at room temperature before measurement. Inductively coupled plasma mass spectrometry (ICP-MS, Xseries II, Thermoscientific, U.S.A.) was used for quantitative determination of levels of platinum. The critical aggregation concentration (CAC) was measured by fluorescence spectrometry that performed on a PTI fluorescence master system with the software Felix 4.1.0.

Critical Aggregation Concentration (CAC). Nile red was used as fluorescence probe to determine the CAC of P(Glu-*co*-Lys) random copolymers, following a procedure described by Ji et al.[37] The Nile red loaded aggregates were diluted with the concentration ranging from 0.5 to 1 × 10^{-6} mg/mL in PB at pH 7.4. Fluorescence measurements were taken at an excitation wavelength of 550 nm and the emission was monitored from 580 to 720 nm.

Drug Loading. Typically, P(Glu-*co*-Lys) (90 mg) was dissolved in 148 mL of water (pH 8.0). The solution was equally divided into three flasks; 5.5, 11.1, and 16.7 mg CDDP were added, respectively. The mixtures were shaken at 37 °C for 72 h in the dark. Free drug was removed by dialysis (MWCO 3500) against deionized water for 24 h (the dialysis medium was changed five times) and followed by lyophilization in the dark to obtain the CDDP/P(Glu-*co*-Lys) nanoparticles. The platinum content in the aggregates was determined by ICP-MS. The drug loading content (DLC %) and drug loading efficiency (DLE %) were calculated by following equation:

$$\text{DLC\%} = \frac{\text{amt of CDDP in nanoparticles}}{\text{amt of drug} - \text{loaded nanoparticles}} \times 100\%$$

$$\text{DLE\%} = \frac{\text{amt of CDDP in nanoparticles}}{\text{total amt of CDDP for loading}} \times 100\%$$

In Vitro Release of CDDP. To determine the drug release of CDDP from CDDP/P(Glu-*co*-Lys) nanoparticles, weighed CDDP/P(Glu-*co*-Lys) nanoparticles were suspended in PBS (pH 7.4) and transferred into a dialysis bag (MWCO 3500 Da). The release experiment was initiated by placing the end-sealed dialysis bag into 28 mL of release medium at 37 °C with constant shaking (100 rpm). At selected time intervals, 1 mL of release media was taken out and replenished with an equal volume of fresh media. The amount of CDDP released was determined using ICP-MS.

Cytotoxicity Assay. The cytotoxicity of the P(Glu-*co*-Lys) copolymers and CDDP/P(Glu-*co*-Lys) nanoparticles was analyzed using methyl thiazolyl tetrazolium (MTT) viability assays toward HeLa cells. The cells were seeded in 96-well culture plates at a density of 10000 cells per well in 100 μL of Dulbecco's modified Eagle's medium (DMEM) containing 10% fetal bovine serum, supplemented with 50 U/mL penicillin and 50 U/mL streptomycin, and incubated at 37 °C in 5% CO_2 atmosphere for 24 h, followed by removing culture medium and adding P(Glu-*co*-Lys)s solution or CDDP/P(Glu-*co*-Lys) nanoparticles (in 200 μL of complete DMEM) with different concentrations (0−0.5 mg/mL). After another 72 h incubation, cell viability was analyzed using MTT and measured in a Bio-Rad 680 microplate reader at a wavelength of 490 nm. Cell viability was calculated as the following equation:

$$\text{cell viability\%} = \frac{A_{\text{sample}}}{A_{\text{control}}} \times 100\%$$

A_{sample} and A_{control} were denoted as absorbance of the sample and control wells, respectively.

Cytotoxicity Assay of CDDP/P(Glu-*co*-Lys) Nanoparticles at pH 7.4 or 6.8. HeLa cells were seeded in 96-well plates at 10000 cells per well in 100 μL of DMEM medium and incubated at 37 °C in 5% CO_2 atmosphere for 24 h. The culture medium was replaced with 100 μL of fresh serum-free DMEM medium containing CDDP/P(Glu-*co*-Lys) nanoparticles at pH 7.4 or 6.8. After a 2 h treatment, the medium was replaced by fresh DMEM at pH 7.4 and further incubated for 22 h followed by addition of 25 μL of MTT stock solution (5 mg mL^{-1} in PBS). After incubation for an additional 2 h, 100 μL of the extraction buffer (20% SDS in 50% DMF, pH 4.7) was added to the wells and incubated for 6 h. The absorbance of the solution was measured at 570 nm using a Bio-Rad 680 microplate reader and cell viability was normalized to that of HeLa cells cultured with blank culture medium.

Uptake of CDDP/P(Glu-*co*-Lys) Nanoparticles at pH 7.4 or 6.8. HeLa cells were seeded in six-well plates at a density of 3 × 10^5 cells per well in 2.5 mL DMEM medium and incubated in a humidified 5% CO_2 atmosphere for 24 h. The original medium was replaced by fresh serum free DMEM (pH 7.4 or 6.8) that were supplemented with CDDP/P(Glu-*co*-Lys) nanoparticles. The cells were incubated for 4 h at 37 °C, and then rinsed with cold PBS (1 mL × 3), and harvested by trypsin treatment. The harvested cells were suspended in 1 mL of PBS. The cell suspensions were centrifuged at 1000 rpm for 4 min at 4 °C. The supernatants were discarded and the cell pellets were washed with 1 mL of PBS. After two cycles of washing and centrifugation, cells were suspended and diluted to a final volume of 1 mL in PBS. Cell numbers were counted, and then the cell suspensions were treated with nitric

dx.doi.org/10.1021/bm400358z | *Biomacromolecules* 2013, 14, 2023−2032

Scheme 1. Synthesis of P(Glu-*co*-Lys) Random Polypeptide

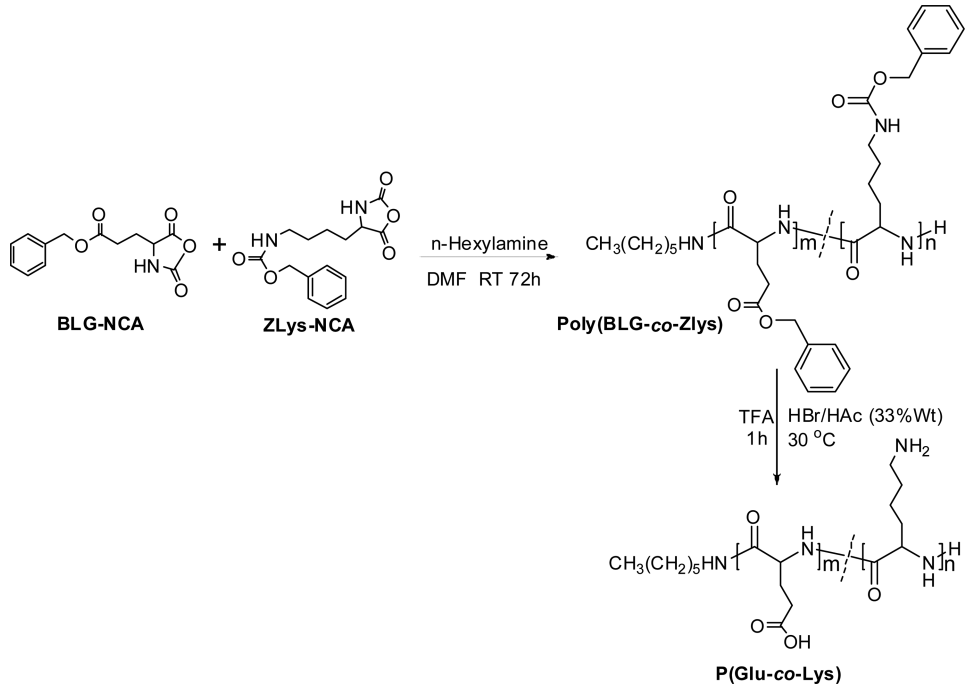

acid (68 vol%) at 70 °C for 12 h. Platinum content analysis was performed using ICP-MS.

Statistical Analysis. Statistical analysis was performed with a Student's *t* test. Statistical significance was assigned for p values <0.05 (95% confidence level).

RESULTS AND DISCUSSION

Synthesis and Characterization of P(Glu-*co*-Lys) Copolymers. Since the syntheses of α-amino acid *N*-carboxyanhydrides (NCAs) were first reported by Hermann Leuchs in 1906,[38] NCA has been widely used as monomer for the ring-opening polymerization to make α-polypeptide. Herein, four P(Glu-*co*-Lys) copolymers were synthesized following the procedure shown in Scheme 1. *n*-Hexylamine was used to initiate the random copolymerization of BLG-NCA and ZLys-NCA, producing poly[(γ-benzyl-L-glutamic acid)-*co*-(3-benzyloxycarbonyl-L-lysine)] [poly(BLG-*co*-ZLys)]. The P(Glu-*co*-Lys) was obtained through the deprotection of the Poly(BLG-*co*-ZLys) in the 7:3 mixture of trifluoroacetic acid HBr/acetic acid (33 wt %) at 30 °C for 1 h. The ^{1}H NMR spectra of P(Glu-*co*-Lys)s were shown in Figure 2. The signals at δ 4.59 and 2.40 ppm with an integral ratio of 1:2 were attributed to the protons of -C***H***< (d) and -C***H***$_2$COOH (f) of glutamic acid moieties, respectively. The protons of -C***H***$_2$CH$_2$COOH (e) of glutamic acid moieties displayed two peaks at δ 2.07 and 1.92 ppm with an integral ratio of 1:1. The signals at δ 4.38, 3.00, and 1.41 − 1.32 ppm are assigned to the protons of -C***H***< (g), -C***H***$_2$NH$_2$ (k), -C***H***$_2$CH$_2$CH$_2$NH$_2$ (i) of lysine moieties, respectively. The signals of protons of >CHC***H***$_2$- (h) and >CHCH$_2$CH$_2$C***H***$_2$- (j) of lysine moieties are overlapped at 1.70−1.61 ppm. The integral ratio of the signals at δ 4.38, 3.00, 1.70−1.61, and 1.41−1.32 ppm is 1:2:4:2. These indicate the existence of glutamic acid and lysine moieties in the obtained copolymers. Signal at δ 6.60 ppm (l) is attributed to the lysine units not glutamic acid units in Figure 2 because the intensity increases with the increase of lysine content in the polypeptides. The proton signal of -NH- of

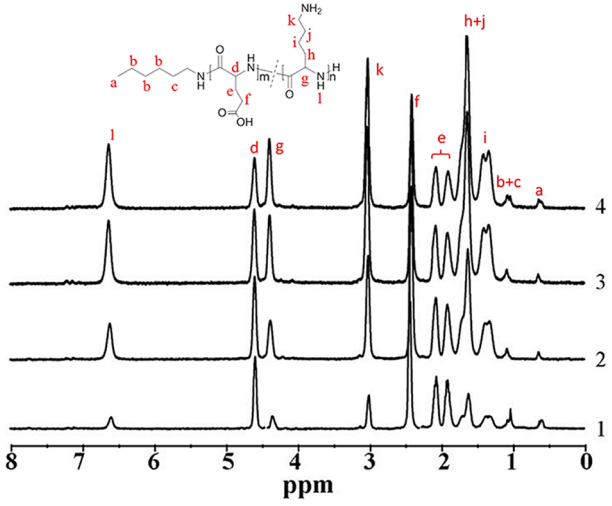

Figure 2. ^{1}H NMR spectra of P(Glu-*co*-Lys)s **1**−**4** in trifluoroacetic acid-*d*.

glutamic acid units "dissapeared" in ^{1}H NMR. Similar phenomenon is observed in the ^{1}H NMR of poly(benzyl L-glutamate) in trifluoroacetic acid-*d* (see Figure S1). The characteristic signal at δ 7.16 ppm of benzene ring protons for poly(BLG-*co*-ZLys) (see Figure S2) has disappeared in the ^{1}H NMR spectra of P(Glu-*co*-Lys)s, which demonstrated the completely removal of protection groups. The methyl groups at the backbone of the P(Glu-*co*-Lys) copolymer displayed two slightly broad signals at δ 50.3 and 49.2 ppm in the ^{13}C NMR spectrum of poly(BLG-*co*-ZLys) (see Figure S3), which implied the formation of a random copolymer. The molar ratio of Glu/Lys was calculated based on the intensities ratio of signals at 2.40 ppm (-C***H***$_2$COOH, f) and 3.00 ppm (-C***H***$_2$NH$_2$, k). The resultant ratio is close to the feed ratio (Table 2). The GPC curves of the four P(Glu-*co*-Lys) copolymers all exhibited unimodal peaks (see Figure S4). The PDIs of the four P(Glu-

dx.doi.org/10.1021/bm400358z | *Biomacromolecules* 2013, 14, 2023−2032

co-Lys) copolymers were in the range of 1.16−1.22 (Table 2), which was rather narrow and indicated the copolymerization was well controllable.

Aggregation of P(Glu-*co*-Lys) Copolymers. The synthesized random P(Glu-*co*-Lys) copolymers could self-assemble into aggregates in PB (pH 7.4). This could be explained as follows. The p*K*a of Glu and Lys units were 4.05 and 10.54, respectively.[34] At pH 7.4, Glu units were negatively charged. Lys units were positively charged. The electrostatic interaction between the oppositely charged units was the driving force for self-assembly to form aggregates.[39] Aggregates formation was also observed for PNiPAM (PLG-*co*-PLLys)s below the lower critical aggregation temperature of the polymer.[34] The CAC was assessed using Nile red as the fluorescent probe.[40] Typical fluorescence emission spectra of Nile red in P(Glu-*co*-Lys) solution (pH 7.4) at different concentrations were shown in Figure 3a. The fluorescence intensity increased when the

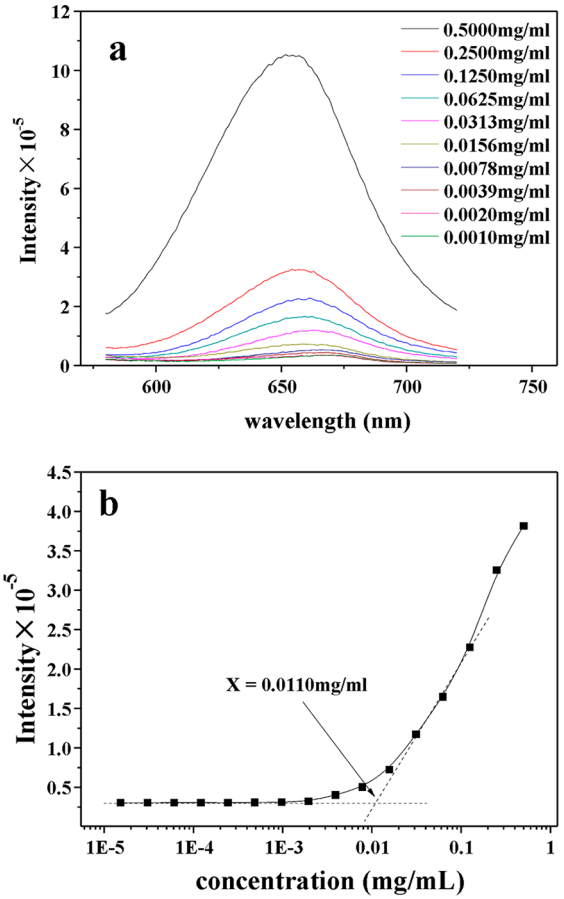

Figure 3. Fluorescence emission spectra of Nile red in aqueous of P(Glu-*co*-Lys) **2** with different concentrations in PB at pH 7.4 (a) and plot of the emission intensity at 650 nm as a function of concentration of P(Glu-*co*-Lys) **2** (b).

concentration of the copolymer rose from 6.125 × 10^{-5} to 0.5 mg/mL. From the plot of the emission intensity at 650 nm as a function of concentration of the P(Glu-*co*-Lys), the CAC value of P(Glu-*co*-Lys) copolymers could be obtained from the intersection of the tangent to the horizontal line of intensity ratio with relatively constant value and the diagonal line with rapidly increased intensity ratio (Figure 3b). The CAC value of the copolymers **1**−**4** in PB at pH 7.4 was 6.3, 11.1, 40.4, and 5.4 × 10^{-3} mg/mL (Figure 4), respectively. The copolymer **3** with

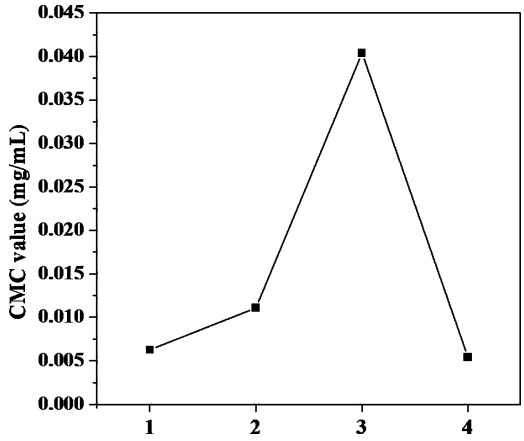

Figure 4. CAC of P(Glu-*co*-Lys) **1**−**4** in PB (pH 7.4).

Glu/Lys molar ratio of 0.97:1 have highest CAC values among the four P(Glu-*co*-Lys)s. This may result from the highest zwitterion content of copolymer **3** among the four P(Glu-*co*-Lys) copolymers.

The hydrodynamic radii (R_h) and morphologies of the aggregates were investigated by DLS and TEM. As shown in Table 2, the R_h of the aggregates of copolymers **1**−**4** in PB of pH 7.4 was 96 ± 30, 113 ± 20, 132 ± 33, and 88 ± 9 nm, respectively. TEM micrograph showed that the P(Glu-*co*-Lys) **1** aggregates took spherical morphology with the average radius around 54 ± 13 nm (Figure 5). The average radii of the P(Glu-

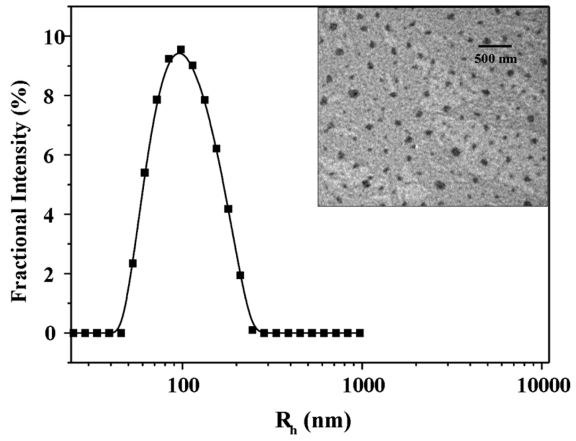

Figure 5. R_h and size distributions of P(Glu-*co*-Lys) **1** aggregates. The inset images were the TEM micrograph of the corresponding aggregates.

co-Lys) **2**−**4** aggregates were around 40 ± 12, 36 ± 5, and 41 ± 9 nm, respectively (Table 2). These were contrast to the R_h values measured by DLS. The hydrodynamic radius measured by DLS was much larger than what TEM showed, suggesting the formation of aggregates.[41] The low resolution of the microscopy and the polydispersity of the nanoparticles may also be responsible for the difference between DLS measurement and TEM.

pH has great influence on the self-assemble of P(Glu-*co*-Lys)s. ^{1}H NMR spectroscopy and DLS were used to check the responsiveness of P(Glu-*co*-Lys) **3** to solution pH (Figure 6). At pH 3.0 and 6.5, the proton signals from lysine residues (δ 2.9 ppm) are visualized in the ^{1}H NMR due to the protonation. In contrast, the signals from the glutamic acid residues (δ 2.3−

dx.doi.org/10.1021/bm400358z | *Biomacromolecules* 2013, 14, 2023−2032

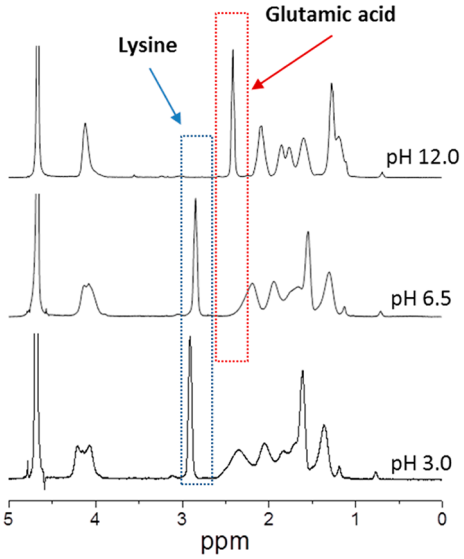

Figure 6. ^{1}H NMR spectra of P(Glu-*co*-Lys) **3** in D_2O at different solution pH values (25 °C).

2.5 ppm) almost disappeared because of the hydrophobicity of the protonated glutamic acid units. At pH 12.0, the proton signals from lysine residues (δ 2.9 ppm) almost disappeared because the lysine residues were deprotonated and became less-soluble in water. Strong proton signals from the glutamic acid residues appeared at δ 2.3−2.5 ppm.[34,35] The P(Glu-*co*-Lys) **3** formed aggregates at low, neutral, and high pH. The size of the aggregates changes with the solution pH (Figure S5). The hydrodynamic radii of P(Glu-*co*-Lys) **3** aggregates are around 94 ± 12 nm at pH 3.5, 132 ± 33 nm at pH 7.4, and 92 ± 9 nm at pH 12.0 in aqueous solution. The size change of the aggregates may be due to the secondary conformation changed from unordered coil at neutral pH to more compact α-helical structure at low pH or high pH (Figure S6).

Surface Charge of P(Glu-*co*-Lys) Aggregates. A key aspect for the P(Glu-*co*-Lys) aggregates was the effect of solution's pH upon surface charge. The change of surface charge with solution's pH was monitored by the relationship of zeta potential and pH value (Figure 7). Because of the existence of carboxyl group and amino group on the P(Glu-*co*-Lys) copolymers, the aggregates were pH-responsive. With the

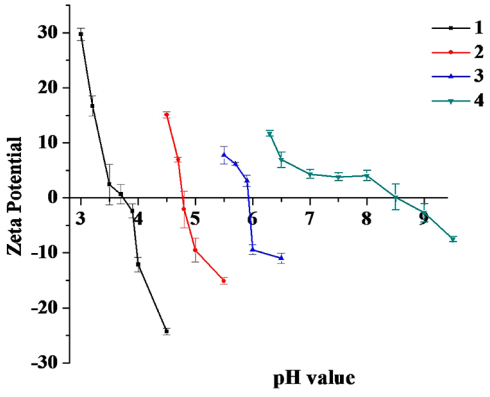

Figure 7. Relationship of pH and zeta potential of aggregates of P(Glu-*co*-Lys) **1**−**4** (Glu/Lys molar ratio of the P(Glu-*co*-Lys)s has great influence on the transition pH at which the surface charge of the P(Glu-*co*-Lys) aggregates reversed).

increase of solution's pH, the zeta potential value of all P(Glu-*co*-Lys) aggregates decreased because of the deprotonation of the copolymers. The Glu/Lys molar ratio of the P(Glu-*co*-Lys)s has great influence on the transition pH at which the surface charge of the P(Glu-*co*-Lys) aggregates reversed. With the increase of the content of lysine moiety, the surface charge of the aggregates reversed at increase pH. In fact, the surface charge of aggregates of copolymer **1** (Glu/Lys = 4.1/1), **2** (Glu/Lys = 1.5/1), **3** (Glu/Lys = 0.97/1), and **4** (Glu/Lys = 1/1.5) reversed at pH 3.7, 4.8, 5.9, and 8.5, respectively (Figure 7). This indicated that the transition pH of P(Glu-*co*-Lys) aggregates can be manipulated by the feed ratio of BLG-NCA and ZLys NCA. The zeta potentials of the aggregates of copolymers **1**−**4** at pH 7.4 were −30.3, −21.8, −15.5, and 4.9 mV (Table 2), respectively. Because of the positive surface charge, polypeptide **4** was unsuitable for tumoral pH_e triggered charge-reversal drug delivery system, only polypeptides **1**−**3** were evaluated in the following experiments.

Preparation of CDDP/P(Glu-*co*-Lys) Nanoparticles. *cis*-Dichlorodiammineplatinum(II) (cisplatin, CDDP), a widely used anticancer drug, was loaded via a simple mixing of CDDP with P(Glu-*co*-Lys)s at different feed ratios in aqueous media. Drug loading contents (DLC) and drug loading efficiencies (DLE) were determined by ICP-MS. Highest DLE (88.6%) was obtained when P(Glu-*co*-Lys) **1** was used as drug carriers (**1**−**1** in Table 3). The DLE decreased with the decrease of Glu/Lys ratio in the P(Glu-*co*-Lys) copolymers (Table 3). This implied that amine groups could compete with platinum ions to complex carboxyl groups of P(Glu-*co*-Lys)s. The platinum-carboxylate complexation could be suppressed by the electrostatic interaction between cationic $-NH_3^+$ and anionic $-COO^-$.

Size, Surface Charge, and in Vitro Release of CDDP/P(Glu-*co*-Lys) Nanoparticles. Size has great influence on the pharmacokinetics and biodistribution of nanomedicine.[42] Typical DLS curve and TEM micrograph of the CDDP/P(Glu-*co*-Lys) nanoparticles were shown in Figure 8. With the incorporation of CDDP into P(Glu-*co*-Lys) copolymer **3**, spherical structure with an average radius around 63 ± 16 nm for CDDP/P(Glu-*co*-Lys) nanoparticles **3**−**2** was seen by TEM. In contrast, the R_h of **3**−**2** from DLS measurement was 127 ± 20 nm (Table 3). The smaller size from TEM observations should be due to the formation of aggregates, low resolution of the microscopy and the polydispersity of the nanoparticles, this was similar to P(Glu-*co*-Lys) aggregates. Compared with the R_h of CDDP/mPEG-*b*-poly(glutamic acid) micelle (radius 14 nm), the R_h of CDDP/P(Glu-*co*-Lys) nanoparticle is much bigger, this may be due to the random nature of the Glu/Lys units in P(Glu-*co*-Lys).

Surface charge is extremely important for a charge-reversal drug delivery system. Because of the consumption of the carboxylate groups by the drug CDDP, an increase in zeta-potential value was observed after drug loading in all cases (Tables 2 and 3). At pH 7.4, the zeta-potential value of P(Glu-*co*-Lys) aggregates was −30.3, −21.8, and −15.5 mV for copolymers **1**−**3**, respectively. After drug loading, the zeta-potential value was increased to −21.0, −19.8, and −10.8 mV for CDDP/P(Glu-*co*-Lys) nanoparticles **1**−**1**, **2**−**1**, and **3**−**1**, respectively. Because both CDDP-loaded nanoparticles **1**−**1** and **2**−**1** were relatively highly negatively charged at both pH 6.8 and 7.4, P(Glu-*co*-Lys) **1** and **2** were not suitable for the tumor pH_e triggered charge-reversal drug delivery. The influence of DLC and solution's pH on the zeta potential of

dx.doi.org/10.1021/bm400358z | *Biomacromolecules* 2013, 14, 2023−2032

Table 3. Properties of CDDP/P(Glu-*co*-Lys) Nanoparticles

nanoparticle	copolymer	feed ratio [CDDP]/ [COOH]	R_h[a] (nm)	DLE[b] (%)	DLC[c] (wt %)	zeta potential at pH 6.8	zeta potential at pH 7.4	IC_{50}[d] (10^{-3} g L^{-1})
1−1	1	5/100	216 ± 48	88.6	14.0	−18.2 ± 2.7	−21.0 ± 1.9	54.4
2−1	2	5/100	224 ± 95	64.4	8.1	−17.8 ± 3.7	−19.8 ± 4.2	24.3
3−1	3	5/100	79 ± 5	16.4	1.8	−7.2 ± 2.4	−10.8 ± 3.1	18.8
3−2	3	12/100	127 ± 20	16.8	2.7	4.2 ± 2.3	−4.9 ± 2.1	13.7
3−3	3	15/100	184 ± 14	17.9	3.9	5.8 ± 3.6	3.3 ± 1.7	11.1

[a]Mean ± standard deviation, determined by DLS. [b]Drug loading efficiency. [c]Drug loading content. [d]Half maximal inhibitory concentration.

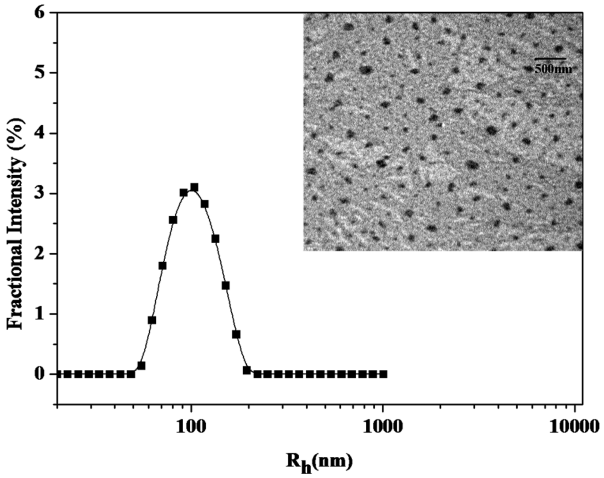

Figure 8. TEM image and DLS characterization of CDDP/P(Glu-*co*-Lys) nanoparticles (**3−2**).

CDDP-loaded systems of **3−1**, **3−2**, and **3−3** was further investigated. As shown in Figure 9, DLC has great influence on the transition pH at which the surface charge of the CDDP-loaded nanoparticles reversed. With the increase of the DLC, the surface charge of the CDDP/P(Glu-*co*-Lys) nanoparticles reversed at pH 6.0, 7.0, and 8.1 for **3−1**, **3−2** and **3−3**, respectively. The transition pH of 7.0 is excellent for a tumor extracellular acidity triggered charge-reversal drug delivery because the tumor extracellular environment is slightly acidic ($pH_e \approx 6.8$). The pH of bloodstream is ~7.4. This indicated that the **3−2** would be negative-charged in the circulation blood (zeta potential, −4.9 mV at pH 7.4), which will minimize the undesirable rapid elimination of CDDP/P(Glu-*co*-Lys) nanoparticles from the blood circulation, and facilitate their accumulation at the tumor sites.[43] The surface charge of **3−2** would change to positive in the tumor extracellular fluid (zeta potential, 4.2 mV at pH 6.8), which would enhance the uptake of CDDP/P(Glu-*co*-Lys) nanoparticles. These indicated **3−2** possessed high potential in the tumor pH_e triggered charge-reversal drug delivery.

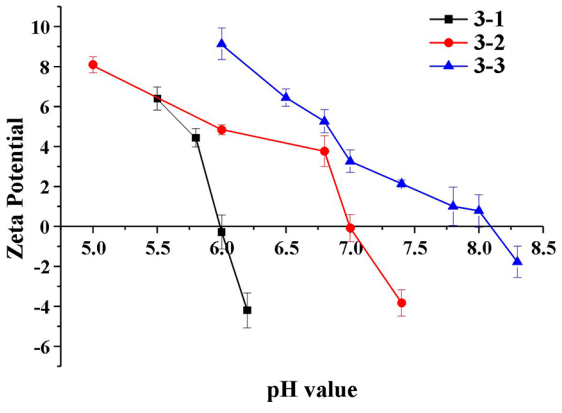

Figure 9. Influence of DLC and pH on the zeta potential of CDDP-loaded nanoparticles of **3−1**, **3−2**, and **3−3**. (DLC has great influence on the transition pH at which the surface charge of the CDDP/P(Glu-*co*-Lys) nanoparticles reversed. This indicated the transition pH of CDDP/P(Glu-*co*-Lys) nanoparticles could be tuned by changing the loaded content of CDDP.)

The in vitro release of CDDP from CDDP/P(Glu-*co*-Lys) nanoparticles were carried out in PBS. Typical release profiles were shown in Figure 10. The release of CDDP was in a controlled and sustained manner; no obvious initial burst release was observed. This indicated that most of the platinum had a high possibility of being contained during the blood circulation. Slightly faster drug release was observed at pH 6.8 than at pH 7.4, which may result from the protonation of carboxylic groups of glutamic acid units, which weakened the complexation of CDDP with carboxylic groups.

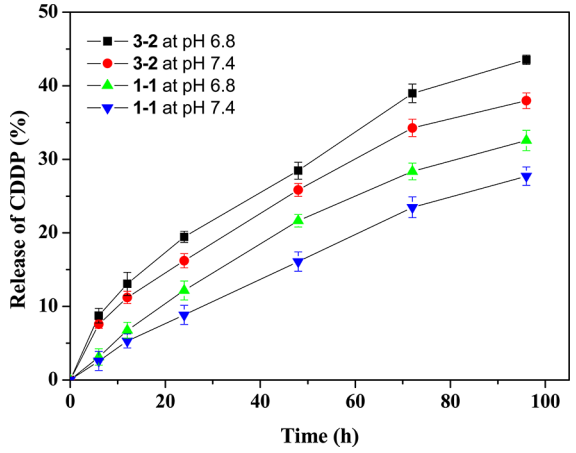

Figure 10. CDDP release from samples **1−1** and **3−2** in PBS at pH 7.4 or 6.8, 37 °C. Each datum represented the average of three independent determinations.

In Vitro Cytotoxicity of P(Glu-*co*-Lys)s and CDDP/P(Glu-*co*-Lys) Nanoparticles. The cytotoxicity of the P(Glu-*co*-Lys) copolymers and CDDP/P(Glu-*co*-Lys) nanoparticles was evaluated by MTT assay against the HeLa cell line using PEI25K as control. As shown in Figure 11, the viabilities of HeLa cells treated with copolymers **1−3** were higher than 85% at concentration from 7.8125×10^{-4} g/L to 0.05 g/L, which indicated copolymers **1−3** were relatively nontoxic to the cells and possessed excellent biocompatibility. The copolymer **4** was found to be toxic to the HeLa cells (cell viabilities were below 50% at copolymer concentration of 0.05 g L^{-1}). These implied that the increased lysine content in the P(Glu-*co*-Lys)s leading

dx.doi.org/10.1021/bm400358z | *Biomacromolecules* 2013, 14, 2023−2032

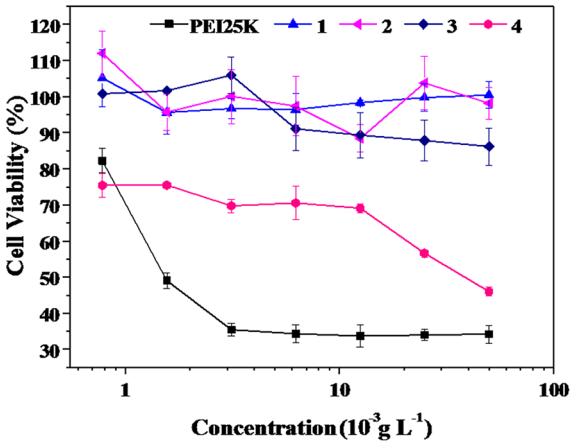

Figure 11. In vitro cytotoxicity of P(Glu-*co*-Lys) copolymers **1**−**4** to HeLa cells using PEI25K as control. Data were expressed as mean ± standard deviation (n = 6).

to more positive charge and resulting in high toxicity and poor biocompatibility.

To evaluate the cytotoxicity of CDDP/P(Glu-*co*-Lys) nanoparticles, free CDDP was used as control. As shown in Figure 12, the CDDP-loaded nanoparticles could effectively

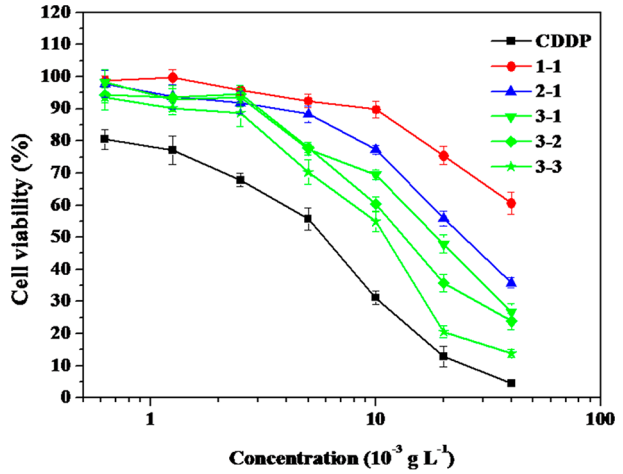

Figure 12. In vitro cytotoxicities of CDDP/P(Glu-*co*-Lys) nanoparticles to HeLa cells with free CDDP as control. Data were expressed as mean ± standard deviation (n = 6).

inhibit the proliferation of HeLa cells but showed relatively lower toxicities compared to free CDDP, which was probably due to the gradual release of CDDP in the cases of CDDP/P(Glu-*co*-Lys) nanoparticles. For the same P(Glu-*co*-Lys) copolymer, the nanoparticles with higher CDDP loading content displayed higher cell toxicities (**3**−**1** < **3**−**2** < **3**−**3**). This could be explained that more carboxylate groups of the P(Glu-*co*-Lys) were complexed, the nanoparticles exhibited more positive charges, which led to the increase of cytotoxicity and the decrease of IC_{50} of drug-loaded nanoparticles (Table 3).

Cytotoxicity and Uptake of CDDP/P(Glu-*co*-Lys) Nanoparticles at pH 7.4 or 6.8. To verify the feasibility of the tumor extracellular pH triggered charge-reversal CDDP/P(Glu-*co*-Lys) nanoparticles **3**−**2** for cancer therapy, cell-proliferation inhibition was tested in vitro at pH 7.4 or 6.8. HeLa cells were incubated with **3**−**2** in fresh serum-free DMEM at pH 7.4 or 6.8 and subjected to an MTT assay. As shown in Figure 13, **3**−**2** showed more inhibition of proliferation of HeLa cells at pH

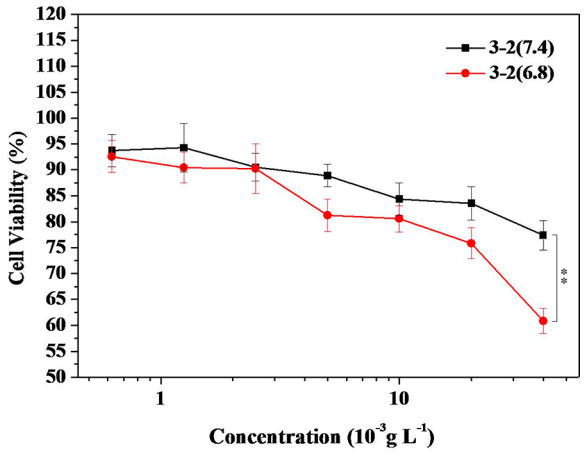

Figure 13. In vitro cytotoxicity of **3**−**2** in a different pH environment. (Before the culture medium was replaced by fresh DMEM at pH 7.4 and incubated for 22 h, HeLa cells were incubated for 2 h in fresh serum-free DMEM medium containing **3**−**2** at pH 7.4 or 6.8. **3**−**2** showed more inhibition of proliferation of HeLa cells at pH 6.8 than at pH 7.4). $^{**}p < 0.01$.

6.8 than at pH 7.4. This phenomenon was also observed by Wang et al. upon the tumor acidity-activated charge conversional, DOX-loaded PAMA-DMMA nanogels.[27] This could be explained that the positively charged **3**−**2** nanoparticles at pH 6.8 are more readily internalized by cells than the negative **3**−**2** nanoparticles at pH 7.4. This was further confirmed by cellular uptake experiments (Figure 14). Compared with the cellular

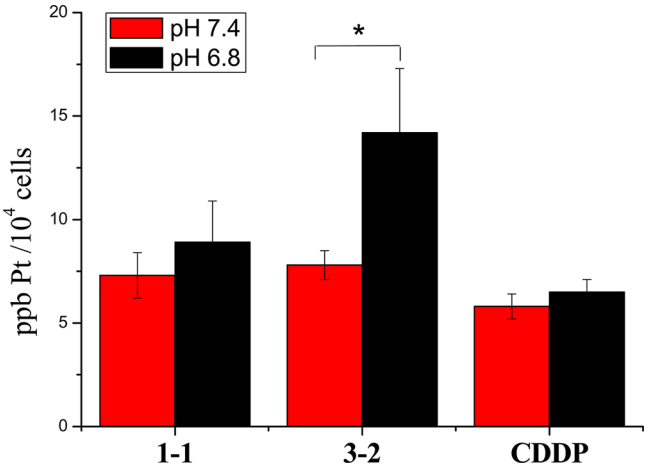

Figure 14. Cellular uptake of the CDDP and CDDP/P(Glu-*co*-Lys) nanoparticles. The data are shown as mean ± SD (n = 4), $^{*}p < 0.05$.

uptake at pH 7.4, remarkably enhanced intracellular uptake was detected at pH 6.8 for tumor pH_e triggered charge-reversal CDDP/P(Glu-*co*-Lys) nanoparticles **3**−**2**, which was in contrast with those of non-charge-reversal CDDP and nanoparticles **1**−**1** where there were no significant difference in the cellular uptake at pH 6.8 and 7.4. If the pH-relevant uptake behavior was caused by a kind of natural behavior transition of Hela cells upon pH changing, Hela cells should significantly uptake more CDDP and **1**−**1** at pH 6.8 than at pH 7.4. But in fact, Hela cells only had significantly more uptake of **3**−**2** at pH

dx.doi.org/10.1021/bm400358z | *Biomacromolecules* 2013, 14, 2023−2032

6.8 than at pH 7.4. This indicated that the pH-relevant uptake behavior was caused by the pH-sensitive nanoparticles.

CONCLUSIONS

Novel tumor extracellular pH-triggered charge-reversal CDDP/P(Glu-*co*-Lys) drug delivery system has been presented. The pH-responsive random polypeptide P(Glu-*co*-Lys)s were successfully synthesized through the ROP of BLG-NCA and ZLys-NCA. Solution's pH, L-glutamic acid/L-lysine ratio and CDDP loading content have great influence on the surface-charge of CDDP/P(Glu-*co*-Lys) nanoparticles. The CDDP/P(Glu-*co*-Lys) nanoparticles (**3**−**2**) with L-glutamic acid/L-lysine molar ratio of 0.97:1 and drug loading content of 2.69% was negatively charged at pH 7.4 (blood pH) and would be transformed to positively charged at pH 6.8 (tumor extracellular pH). The charge reversal enhanced the uptake of the CDDP/P(Glu-*co*-Lys) nanoparticles and the efficiency in inhibiting the proliferation of cancer cells. This indicated that the CDDP/P(Glu-*co*-Lys) was a potential tumor extracellular pH triggered charge-reversal drug delivery systems for cancer therapy.

ASSOCIATED CONTENT

Supporting Information

^{1}H NMR spectra of poly(benzyl L-glutamate) and poly(BLG-*co*-ZLys), ^{13}C NMR spectrum of P(Glu-*co*-Lys), GPC curves of P(Glu-*co*-Lys) copolymers, hydrodynamic radius, and circular dichroism of P(Glu-*co*-Lys) **3** in aqueous solution at different pH. This material is available free of charge via the Internet at http://pubs.acs.org.

AUTHOR INFORMATION

Corresponding Author

*E-mail: ztang@ciac.jl.cn (Z.T.); zxf7515@yahoo.com.cn (X.Z.).

Notes

The authors declare no competing financial interest.

ACKNOWLEDGMENTS

This research was financially supported by National Natural Science Foundation of China (Projects 21004061, 51173184, 51233004, 51021003, 51273169, and 21104076), Ministry of Science and Technology of China (International Cooperation and Communication Program 2011DFR51090), Knowledge Innovation Program of the Chinese Academy of Sciences (Grant No. KJCX2-YW-H19).

REFERENCES

(1) Devadasu, V. R.; Bhardwaj, V.; Kumar, M. N. V. R. Can controversial nanotechnology promise drug delivery? *Chem. Rev.* **2013**, *113* (3), 1686−735.

(2) Oh, J. K.; Drumright, R.; Siegwart, D. J.; Matyjaszewski, K. The development of microgels/nanogels for drug delivery applications. *Prog. Polym. Sci.* **2008**, *33* (4), 448−477.

(3) Peer, D.; Karp, J. M.; Hong, S.; FarokHzad, O. C.; Margalit, R.; Langer, R. Nanocarriers as an emerging platform for cancer therapy. *Nat. Nanotechnol.* **2007**, *2* (12), 751−760.

(4) Meng, F. H.; Zhong, Z. Y.; Feijen, J. Stimuli-responsive polymersomes for programmed drug delivery. *Biomacromolecules* **2009**, *10* (2), 197−209.

(5) Bajpai, A.; Shukla, S.; Saini, R. *Stimuli Responsive Drug Delivery Systems: From Introduction to Application*. Smithers Rapra Publishing: Akron, OH, 2010.

(6) Fleige, E.; Quadir, M. A.; Haag, R. Stimuli-responsive polymeric nanocarriers for the controlled transport of active compounds: Concepts and applications. *Adv. Drug Delivery Rev.* **2012**, *64* (9), 866−884.

(7) Lee, E. S.; Gao, Z.; Bae, Y. H. Recent progress in tumor pH targeting nanotechnology. *J. Controlled Release* **2008**, *132* (3), 164−170.

(8) Song, W.; Tang, Z.; Li, M.; Lv, S.; Yu, H.; Ma, L.; Zhuang, X.; Huang, Y.; Chen, X. Tunable pH-sensitive poly(β-amino ester)s synthesized from primary amines and diacrylates for intracellular drug delivery. *Macromol. Biosci.* **2012**, *12* (10), 1375−1383.

(9) Petros, R. A.; Ropp, P. A.; DeSimone, J. M. Reductively labile PRINT particles for the delivery of doxorubicin to HeLa cells. *J. Am. Chem. Soc.* **2008**, *130* (15), 5008−5009.

(10) Li, Y.-L.; Zhu, L.; Liu, Z.; Cheng, R.; Meng, F.; Cui, J.-H.; Ji, S.-J.; Zhong, Z. Reversibly stabilized multifunctional dextran nanoparticles efficiently deliver doxorubicin into the nuclei of cancer cells. *Angew. Chem., Int. Ed.* **2009**, *48* (52), 9914−9918.

(11) Nishiyama, N.; Yokoyama, M.; Aoyagi, T.; Okano, T.; Sakurai, Y.; Kataoka, K. Preparation and characterization of self-assembled polymer−metal complex micelle from *cis*-dichlorodiammineplatinum-(II) and poly(ethylene glycol)−poly(α,β-aspartic acid) block copolymer in an aqueous medium. *Langmuir* **1999**, *15* (2), 377−383.

(12) Xiong, Y.; Jiang, W.; Shen, Y.; Li, H.; Sun, C.; Ouahab, A.; Tu, J. A poly(γ,l-glutamic acid)-citric acid based nanoconjugate for cisplatin delivery. *Biomaterials* **2012**, *33* (29), 7182−7193.

(13) Yokoyama, M.; Okano, T.; Sakurai, Y.; Suwa, S.; Kataoka, K. Introduction of cisplatin into polymeric micelle. *J. Controlled Release* **1996**, *39* (2−3), 351−356.

(14) Khandare, J. J.; Jayant, S.; Singh, A.; Chandna, P.; Wang, Y.; Vorsa, N.; Minko, T. Dendrimer versus linear conjugate: influence of polymeric architecture on the delivery and anticancer effect of paclitaxel. *Bioconjugate Chem.* **2006**, *17* (6), 1464−1472.

(15) Calderón, M.; Quadir, M. A.; Strumia, M.; Haag, R. Functional dendritic polymer architectures as stimuli-responsive nanocarriers. *Biochimie* **2010**, *92* (9), 1242−1251.

(16) Priya, B.; Viness, P.; Yahya, E. C.; Lisa, C. d. T. Stimuli-responsive polymers and their applications in drug delivery. *Biomed. Mater.* **2009**, *4* (2), 022001.

(17) Maxfield, F. R.; McGraw, T. E. Endocytic recycling. *Nat. Rev. Mol. Cell. Biol.* **2004**, *5* (2), 121−132.

(18) Watson, P.; Jones, A. T.; Stephens, D. J. Intracellular trafficking pathways and drug delivery: fluorescence imaging of living and fixed cells. *Adv. Drug Delivery Rev.* **2005**, *57* (1), 43−61.

(19) Lee, Y.; Fukushima, S.; Bae, Y.; Hiki, S.; Ishii, T.; Kataoka, K. A protein nanocarrier from charge-conversion polymer in response to endosomal pH. *J. Am. Chem. Soc.* **2007**, *129* (17), 5362−+.

(20) Lee, Y.; Miyata, K.; Oba, M.; Ishii, T.; Fukushima, S.; Han, M.; Koyama, H.; Nishiyama, N.; Kataoka, K. Charge-conversion ternary polyplex with endosome disruption moiety: A technique for efficient and safe gene delivery. *Angew. Chem., Int. Ed.* **2008**, *47* (28), 5163−5166.

(21) Xu, P. S.; Van Kirk, E. A.; Zhan, Y. H.; Murdoch, W. J.; Radosz, M.; Shen, Y. Q. Targeted charge-reversal nanoparticles for nuclear drug delivery. *Angew. Chem., Int. Ed.* **2007**, *46* (26), 4999−5002.

(22) Zhou, Z. X.; Shen, Y. Q.; Tang, J. B.; Fan, M. H.; Van Kirk, E. A.; Murdoch, W. J.; Radosz, M. Charge-reversal drug conjugate for targeted cancer cell nuclear drug delivery. *Adv. Funct. Mater.* **2009**, *19* (22), 3580−3589.

(23) Zhou, Z. X.; Shen, Y. Q.; Tang, J. B.; Jin, E. L.; Ma, X. P.; Sun, Q. H.; Zhang, B.; Van Kirk, E. A.; Murdoch, W. J. Linear polyethyleneimine-based charge-reversal nanoparticles for nuclear-targeted drug delivery. *J. Mater. Chem.* **2011**, *21* (47), 19114−19123.

(24) Miller, C. R.; Bondurant, B.; McLean, S. D.; McGovern, K. A.; O'Brien, D. F. Liposome−cell interactions in vitro: Effect of liposome surface charge on the binding and endocytosis of conventional and sterically stabilized liposomes. *Biochemistry* **1998**, *37* (37), 12875−12883.

(25) Gratton, S. E. A.; Ropp, P. A.; Pohlhaus, P. D.; Luft, J. C.; Madden, V. J.; Napier, M. E.; DeSimone, J. M. The effect of particle design on cellular internalization pathways. *Proc. Natl. Acad. Sci. U.S.A.* **2008**, *105* (33), 11613−11618.
(26) Mailander, V.; Landfester, K. Interaction of nanoparticles with cells. *Biomacromolecules* **2009**, *10* (9), 2379−2400.
(27) Du, J. Z.; Sun, T. M.; Song, W. J.; Wu, J.; Wang, J. A tumor-acidity-activated charge-conversional nanogel as an intelligent vehicle for promoted tumoral-cell uptake and drug delivery. *Angew. Chem., Int. Ed.* **2010**, *49* (21), 3621−3626.
(28) Lee, H. J.; Pardridge, W. M. Monoclonal antibody radiopharmaceuticals: Cationization, pegylation, radiometal chelation, pharmacokinetics, and tumor imaging. *Bioconjugate Chem.* **2003**, *14* (3), 546−553.
(29) Cho, E. C.; Xie, J. W.; Wurm, P. A.; Xia, Y. N. Understanding the role of surface charges in cellular adsorption versus internalization by selectively removing gold nanoparticles on the cell surface with a I-2/KI etchant. *Nano Lett.* **2009**, *9* (3), 1080−1084.
(30) Sethuraman, V. A.; Bae, Y. H. TAT peptide-based micelle system for potential active targeting of anti-cancer agents to acidic solid tumors. *J. Controlled Release* **2007**, *118* (2), 216−224.
(31) Taurin, S.; Nehoff, H.; Greish, K. Anticancer nanomedicine and tumor vascular permeability; Where is the missing link? *J. Controlled Release* **2012**, *164* (3), 265−275.
(32) Deming, T. J. Synthetic polypeptides for biomedical applications. *Prog. Polym. Sci.* **2007**, *32* (8−9), 858−875.
(33) Choe, U.-J.; Sun, V.; Tan, J.-K.; Kamei, D., Self-Assembled Polypeptide and Polypeptide Hybrid Vesicles: From Synthesis to Application. In *Peptide-Based Materials*; Deming, T., Ed.; Springer: Berlin, Heidelberg, 2012; Vol. *310*, pp 117−134.
(34) Li, J. G.; Wang, T.; Wu, D. L.; Zhang, X. Q.; Yan, J. T.; Du, S.; Guo, Y. F.; Wang, J. T.; Zhang, A. Stimuli-responsive zwitterionic block copolypeptides: Poly(*N*-isopropylacrylamide)-*block*-poly(lysine-*co*-glutamic acid). *Biomacromolecules* **2008**, *9* (10), 2670−2676.
(35) Rodriguez-Hernandez, J.; Lecommandoux, S. Reversible inside-out micellization of pH-responsive and water-soluble vesicles based on polypeptide diblock copolymers. *J. Am. Chem. Soc.* **2005**, *127* (7), 2026−2027.
(36) Ding, J. X.; Zhuang, X. L.; Xiao, C. S.; Cheng, Y. L.; Zhao, L.; He, C. L.; Tang, Z. H.; Chen, X. S. Preparation of photo-cross-linked pH-responsive polypeptide nanogels as potential carriers for controlled drug delivery. *J. Mater. Chem.* **2011**, *21* (30), 11383−11391.
(37) Chen, C.; Liu, G.; Liu, X.; Pang, S.; Zhu, C.; Lv, L.; Ji, J. Photo-responsive, biocompatible polymeric micelles self-assembled from hyperbranched polyphosphate-based polymers. *Polym. Chem.* **2011**, *2* (6), 1389−1397.
(38) Leuchs, H. Ueber die Glycin-carbonsäure. *Ber. Dtsch. Chem. Ges.* **1906**, *39* (1), 857−861.
(39) Agut, W.; Brûlet, A.; Schatz, C.; Taton, D.; Lecommandoux, S. B. pH and Temperature Responsive Polymeric Micelles and Polymersomes by Self-Assembly of Poly[2-(dimethylamino)ethyl methacrylate]-b-Poly(glutamic acid) Double Hydrophilic Block Copolymers. *Langmuir* **2010**, *26*, 10546−10554.
(40) Mynar, J. L.; Goodwin, A. P.; Cohen, J. A.; Ma, Y.; Fleming, G. R.; Frechet, J. M. J. Two-photon degradable supramolecular assemblies of linear-dendritic copolymers. *Chem. Commun.* **2007**, *20*, 2081−2082.
(41) Gohy, J. F.; Hofmeier, H.; Alexeev, A.; Schubert, U. S. Aqueous micelles from supramolecular graft copolymers. *Macromol. Chem. Phys.* **2003**, *204* (12), 1524−1530.
(42) Euliss, L. E.; DuPont, J. A.; Gratton, S.; DeSimone, J. M. Imparting size, shape, and composition control of materials for nanomedicine. *Chem. Soc. Rev.* **2006**, *35* (11), 1095−1104.
(43) Xiao, K.; Li, Y. P.; Luo, J. T.; Lee, J. S.; Xiao, W. W.; Gonik, A. M.; Agarwal, R. G.; Lam, K. S. The effect of surface charge on in vivo biodistribution of PEG-oligocholic acid based micellar nanoparticles. *Biomaterials* **2011**, *32* (13), 3435−3446.